



# High-Efficiency Flexible Organic Photovoltaics and Thermoelectricities Based on Thionyl Chloride Treated PEDOT:PSS Electrodes

Juanyong Wan<sup>1,2†</sup>, Xi Fan<sup>1\*†</sup>, Yunfei Li<sup>1,3</sup>, Pengcheng Li<sup>3</sup>, Ting Zhang<sup>1\*</sup>, Kwun Nam Hui<sup>4</sup>, Huihui Huang<sup>2</sup>, Kai Kang<sup>1</sup> and Lei Qian<sup>1</sup>

<sup>1</sup>Division of Functional Materials and Nanodevices, Ningbo Institute of Materials Technology and Engineering, Chinese Academy of Sciences, Ningbo, China, <sup>2</sup>School of Physics and Electronics, Hunan University, Changsha, China, <sup>3</sup>Hubei Key Laboratory of Plasma Chemistry and Advanced Materials, Hubei Engineering Technology Research Center of Optoelectronic and New Energy Materials, School of Materials Science and Engineering, Wuhan Institute of Technology, Wuhan, China, <sup>4</sup>Joint Key Laboratory of the Ministry of Education, Institute of Applied Physics and Materials Engineering, University of Macau, Taipa, Macau SAR, China

## OPEN ACCESS

### Edited by:

Xi Zhang,  
Shenzhen University, China

### Reviewed by:

Qinglin Jiang,  
South China University of Technology,  
China  
Congcong Liu,  
Jiangxi Science and Technology  
Normal University, China

### \*Correspondence:

Xi Fan  
fanxi@nimte.ac.cn  
Ting Zhang  
zhangting@nimte.ac.cn

<sup>†</sup>These authors have contributed  
equally to this work

### Specialty section:

This article was submitted to  
Physical Chemistry and Chemical  
Physics,  
a section of the journal  
Frontiers in Chemistry

Received: 02 November 2021

Accepted: 21 December 2021

Published: 01 March 2022

### Citation:

Wan J, Fan X, Li Y, Li P, Zhang T,  
Hui KN, Huang H, Kang K and Qian L  
(2022) High-Efficiency Flexible Organic  
Photovoltaics and Thermoelectricities  
Based on Thionyl Chloride Treated  
PEDOT:PSS Electrodes.  
Front. Chem. 9:807538.  
doi: 10.3389/fchem.2021.807538

Conducting polymers have received tremendous attentions owing to their great potentials to harvest both luminous and thermal energies. Here, we reported a flexible transparent electrode of poly(3,4-ethylenedioxythiophene):poly(styrenesulfonate) (PEDOT:PSS) with highly electrical conductivity and raised Seebeck coefficient *via* thionyl chloride treatments. The comprehensive studies of optical, electrical, morphological, structural, and thermoelectrical properties, work function, and stability of the PEDOT:PSS transparent electrodes were systematically evaluated and described. On the basis of the PEDOT:PSS transparent electrodes, the resultant flexible organic solar cells yielded a high power conversion efficiency of 15.12%; meanwhile, the flexible thermoelectricities exhibited the raised power factor of 115.9  $\mu\text{W m}^{-1} \text{K}^{-2}$ , which outperformed the four kinds of rigid thermoelectricities with conventional acid and base treatments.

**Keywords:** flexible transparent electrode, organic solar cell, thermoelectricity, PEDOT:PSS, conducting polymer

## INTRODUCTION

Developments of energy harvesting electronics such as flexible organic solar cells (OSCs) (Sun et al., 2019; Qu et al., 2020; Yao et al., 2020; Chen et al., 2020) and thermoelectricities (TEs) (Park et al., 2014; Xiong et al., 2015; Fan et al., 2017; Li et al., 2019; Jiang et al., 2020) have attracted a great deal of attentions recently. Flexible OSCs, which convert the luminous energy to electricity, have the wearable, portable, and light-weight advantages for a promising application into self-powered smart electronics; whereas flexible TEs, which convert the waste thermal energy to electricity, can be attached to surfaces dissipating heats for electricity generation. As a key device component, the flexible transparent electrode and thermoelectric layer of poly(3,4-ethylenedioxythiophene):poly(styrenesulfonate) (PEDOT:PSS) have the striking virtues, such as aqueous solution manufacturing, low cost, high conductivity ( $\sigma$ ), adjustable work function, and good thermal stability, thereby enabling a promising adaptation of them into flexible OSCs and flexible TEs (Na et al., 2008; Kim et al., 2011; Xia et al., 2012; Kim et al., 2014; Fan et al., 2015; Meng et al., 2015; Worfolk et al., 2015; Song et al., 2018; Fan et al., 2019; Fan, 2021; Wan et al., 2020a; Wan et al., 2020b; Wen et al., 2021; Wan et al., 2021).

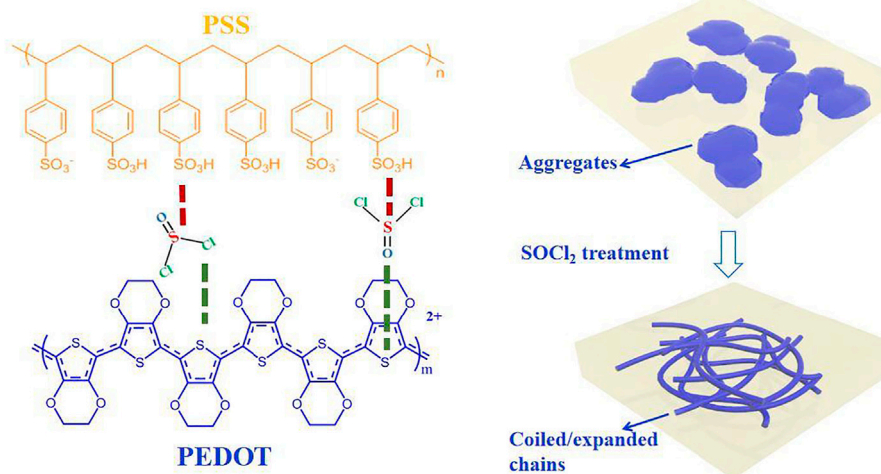


**FIGURE 1** | Schematic diagrams of inter-molecular interactions among PEDOT, PSS, and  $\text{SOCl}_2$ , and morphology evolution of the PEDOT:PSS films induced by  $\text{SOCl}_2$ .

As the most commercial conducting polymers (CPs), PEDOT:PSS (Clevios PH1000) transparent electrodes exhibited a highly electrical conductivity over  $3,000 \text{ S cm}^{-1}$  via strong acid treatments (Xia et al., 2012; Fan et al., 2015). The electrical conductivity was substantially improved after 1) diluted strong acid treatments at high temperatures and 2) fully concentrated strong acid treatments. However, the PEDOT:PSS transparent electrodes coated on plastic substrates suffered from these drawbacks, including inhomogeneous morphology with high roughness, large-domain aggregates with sizes of 30–50 nm in matrices, and limited flexibility (Fan et al., 2015; Fan et al., 2020; Wan et al., 2020a). These factors presumably restrain the power conversion efficiency (PCE) of indium tin oxide (ITO)-free flexible OSCs.

PEDOT:PSS has been also employed as thermoelectric materials (Park et al., 2014; Xiong et al., 2015; Fan et al., 2017; Li et al., 2019; Xu et al., 2021). The power factor (PF) of TEs is defined as  $\text{PF} = S^2\sigma$ , where  $S$  is the Seebeck coefficient (Tritt and Subramanian, 2006; Snyder and Toberer, 2008). To improve the PF of the PEDOT:PSS electrodes, strong acid treatments were commonly employed; however, the strong acid approach commonly result in a rather low PF no more than  $58.7 \mu\text{W m}^{-1} \text{K}^{-2}$ . To improve the thermoelectric performance of the PEDOT:PSS electrodes, a few methods including 1) secondary polar solvent and base multistep treatments, 2) acid and base multistep treatments, and 3) hybrid strategies had been subsequently developed. It should be mentioning that the base treatments employed not only made the processing procedure more complex but also led to a deeply blue PEDOT:PSS thin film, thereby unsuitable to make transparent PEDOT:PSS electrodes.

Thionyl chloride ( $\text{SOCl}_2$ ) molecules involve rich sulfur-chlorine (S-Cl) and sulfur = oxygen (S=O) polar covalent bonds. The polar  $\text{SOCl}_2$  molecules potentially reduce the Coulomb attractions between PEDOT and PSS for a highly electrical conductivity (see inter-molecular interactions in

**Figure 1**). The polar covalent bonds also polarize the conducting PEDOTs for raising the work function ( $\Phi$ ) of the PEDOT:PSS films. A high  $\Phi$  minimizes the energy level mismatch among the PEDOT:PSS anodes, hole transporting layers (HTLs), and electron donors of photo-active layer of OSCs for an efficient charge transport. Therefore, the  $\text{SOCl}_2$ -treated PEDOT:PSS electrodes maybe suitable for flexible ITO-free OSCs and TEs.

Herein, we propose the  $\text{SOCl}_2$  treatment to energetically raise the electrical conductivity, Seebeck coefficient, and work function of the PEDOT:PSS electrodes. The  $\text{SOCl}_2$  treatment did lead to a smooth, uniform, and homogeneous PEDOT:PSS electrode that consisted of expanded/coiled chains (see morphology evolution in **Figure 1**). The electrical conductivity and work function was raised to  $2,230 \text{ S cm}^{-1}$  and  $4.89 \text{ eV}$ , respectively. The solution-processed flexible OSCs yielded a considerably high PCE of 15.12%, which was comparable to that of the rigid OSCs with 110-nm-thick ITO-coated glass substrates. Meanwhile, the flexible TEs exhibited a high Seebeck coefficient of  $22.8 \mu\text{V K}^{-1}$  and PF of  $115.9 \mu\text{W m}^{-1} \text{K}^{-2}$  with highly optical transmittance. The work demonstrates the synergistic enhancements in  $\sigma$ ,  $S$ , and  $\Phi$  of PEDOT:PSS electrodes by  $\text{SOCl}_2$  and the promising applications into flexible energy harvesting electronics.

## EXPERIMENTAL

### Materials

PM6 and Y6 were purchased from Solarmer Materials Inc., Beijing. PEDOT:PSS aqueous solutions (Clevios PH1000 and P VP A14083) were purchased from Heraeus, Germany.

### Solar Cell Fabrication

For the rigid ITO-based solar cells, glass substrates (size:  $2.0 \text{ cm} \times 2.0 \text{ cm}$ ) were cleaned through using ultrasonic treatments in deionized (DI) water, acetone, and isopropyl alcohol (IPA)

and then were processed in UV-ozone chambers for 10 min. For the flexible solar cells, the polyethylene terephthalate (PET) plastic substrates were cleaned by IPA followed by baking at 100°C for 10 min. Next, PEDOT:PSS aqueous solutions (PH1000) were filtered through 0.45- $\mu\text{m}$  syringe filter. The PEDOT:PSS (PH1000) solutions were spin-coated on underlying substrates at 3,500 rpm, and the as-cast PEDOT:PSS films were dried at 80°C for 15 min in the air atmosphere. The spin-coating deposition of PEDOT:PSS (PH1000) and the drying treatment at 80°C were conducted again. Then, the  $\text{SOCl}_2$  soaking treatment was conducted *via* dipping the >99 wt.%  $\text{SOCl}_2$  solutions on the PEDOT:PSS surfaces at room temperature. Upon the  $\text{SOCl}_2$  treatment for 10 min, the  $\text{SOCl}_2$  residues were washed off by DI water and IPA followed by baking at 80°C for 15 min.

Subsequently, a PEDOT:PSS HTL (Clevios P VP AI4083) was spin-coated on the ITO and PEDOT:PSS electrodes at 3,000 rpm for 30 s, and the HTL was dried at 100°C for 10 min. After that, the photo-active layer blends of PM6:Y6 were dissolved in chloroform with 1-chloronaphthalene (0.5%, v/v) and were spin-coated at 3,000 rpm for 30 s on the PEDOT:PSS (P VP AI4083) HTL. Then, perylene diimide amino N-oxide (PDINO) in methanol (1.0 mg  $\text{ml}^{-1}$ ) were spin-coated on the surfaces of photo-active layers at 2,000 rpm to obtain the electron transporting layers. Finally, the cathodes of Al were thermally evaporated under a pressure at  $10^{-4}$  Pa. The active area is 4.00  $\text{mm}^2$ . Note that metal probes were contacted with Al top cathodes and the PEDOT:PSS bottom anodes coated with silver (Ag) pastes for the current density–voltage ( $J$ – $V$ ) characteristics.

## Thermoelectricity Fabrication

PEDOT:PSS aqueous solutions (Clevios PH1000) were filtered through 0.45- $\mu\text{m}$  syringe filter. The PH1000 solutions were spin-coated on the clean PET substrates at 3,500 rpm followed by the drying at 80°C for 15 min in the air atmosphere. The spin coating of PH1000 and the drying treatment were conducted again. Subsequently, the sulfuric acid ( $\text{H}_2\text{SO}_4$ ) and methanesulfonic acid ( $\text{CH}_3\text{SO}_3\text{H}$ ) treatments were conducted *via* dipping these acid solutions on the PEDOT:PSS surfaces with a controlled temperature of 140°C or room temperature, respectively; whereas the  $\text{SOCl}_2$  treatment was conducted *via* dipping the  $\text{SOCl}_2$  solution on the PEDOT:PSS surfaces at room temperature. Upon the treatments for 10 min, the acid and  $\text{SOCl}_2$  residues were washed off by DI water and IPA followed by baking at 80°C for 15 min. In the following base treatment, 0.1 M NaOH aqueous solutions (100  $\mu\text{l}$ ) were dropped onto the acid-treated PEDOT:PSS films. The NaOH base treatment was conducted for 1 min at room temperature. The as-treated films were rinsed with DI water for three times followed by drying on a hot plate at 100°C for 5 min. Finally, two Ag line electrodes with a length of 1.5 cm and a distance of 2 mm were prepared *via* using Ag pastes.

## Characterizations

Sheet resistance was measured through using the van der Pauw method. Film thickness was conducted by a surface profile meter (TalySurf Series II). UV–vis spectra were taken on GS54T spectrophotometers (Shanghai Lengguang Technology Co., China). Film morphology was conducted using scanning probe

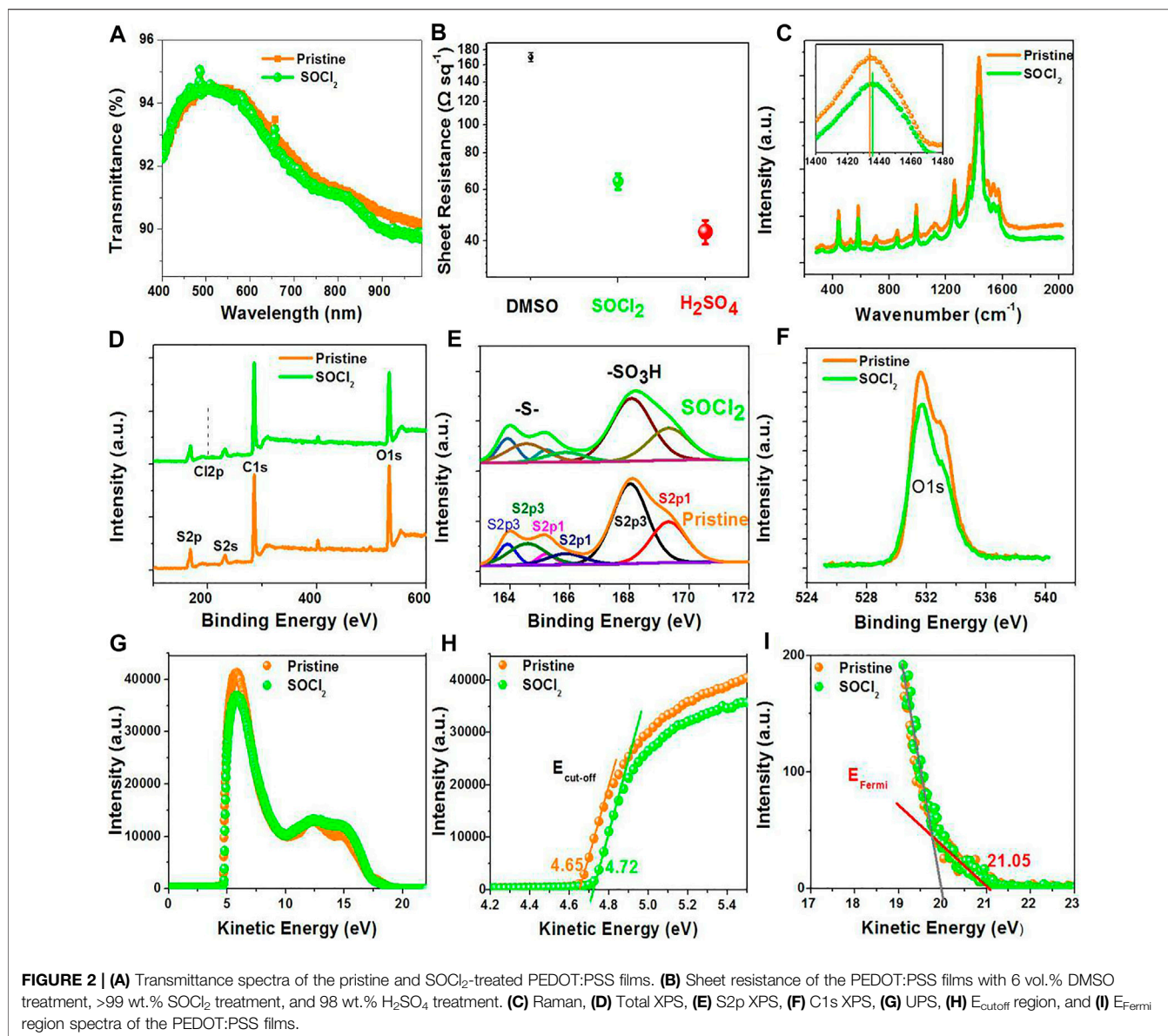
microscope (SPM, VEECO Dimension 3100V). Element compositions of the PEDOT:PSS films were conducted by X-ray photoelectron spectroscopy (XPS, XSAM800). UV photoelectron spectra (UPS) measurements were carried out using a Kratos AXIS ULTRA DALD UPS system. The  $J$ – $V$  characteristics were measured in the nitrogen ( $\text{N}_2$ )–filled glove boxes using a Keithley 2400 sourceMeter under the illumination of AM 1.5G, with a AAA solar simulator (Newport, model 94023A). The lamp was calibrated by a 2 cm  $\times$  2 cm monocrystalline silicon reference cell (KG5 filter) provided by Newport Corporation. The light intensity was calibrated with a standard silicon detector. External quantum efficiency (EQE) was conducted through the Newport quantum efficiency measurement system (ORIEL IQE 200TM) in the ambient atmosphere. The light intensity was calibrated with a standard Si/Ge solar cell.

The Seebeck coefficient was measured by using a home-built system as previously reported in the previous literature 10. One side of the film was heated up by the Peltier device as hot end, whereas the other side was maintained in atmosphere as cold end. The temperature gradient ( $\Delta T$ ) was measured by  $T$ -type thermocouples and varied  $\Delta T$  could be generated by controlling the applied power for the Peltier device. Thermoelectric voltage ( $\Delta V$ ) was obtained by using a Keithley 2000 multimeter, and the slope of the linear fitting of  $\Delta V$ – $\Delta T$  plots was calculated to be the Seebeck coefficient.

## RESULTS AND DISCUSSION

### Opt-Electrical Characteristics of PEDOT:PSS Films

The fundamental investigations of the PEDOT:PSS thin films with  $\text{SOCl}_2$  treatments are systematically introduced. The  $\text{SOCl}_2$  approach boosts the electrical conductivity, work function, Seebeck coefficient as well as stability, and directly links to the underlying mechanism of the enhanced PCE for flexible OSCs and the improved PF for flexible TEs. **Figures 2A,B** show the optical transparency ( $T\%$ ) and sheet resistance ( $R_{\text{sh}}$ ) of the pristine PEDOT:PSS thin film and the PEDOT:PSS electrodes (70-nm thickness) with the  $\text{SOCl}_2$  treatment at room temperature, respectively. After the  $\text{SOCl}_2$  treatment,  $T\%$  was slightly decreased from 94.4 to 94.3% at  $\lambda = 550$  nm and from 90.6 to 90.0% at  $\lambda = 900$  nm, which were accompanied with a morphology evolution of the PEDOT:PSS electrodes. A high optical transmittance was generally achieved *via* improving the oxidation levels of PEDOT molecules and/or largely reducing the insulating and hydrophilic PSS components (Khan et al., 2015; Reyes-Reyes and Lopez-Sandoval, 2018). Here, the transmittance results suggest no visible raise of the oxidation levels of the PEDOTs by the  $\text{SOCl}_2$  treatment. Upon the  $\text{SOCl}_2$  treatment, the PEDOT:PSS electrodes showed a  $R_{\text{sh}}$  of 64  $\Omega \text{sq}^{-1}$ , which was much lower than that (170  $\Omega \text{sq}^{-1}$ ) of the conventional PEDOT:PSS ones with 6 vol.% dimethyl sulfoxide (DMSO) treatments and higher than that (43  $\Omega \text{sq}^{-1}$ ) of the PEDOT:PSS ones with 98 wt.%  $\text{H}_2\text{SO}_4$  treatments. Note that 98 wt.%  $\text{H}_2\text{SO}_4$  treatments



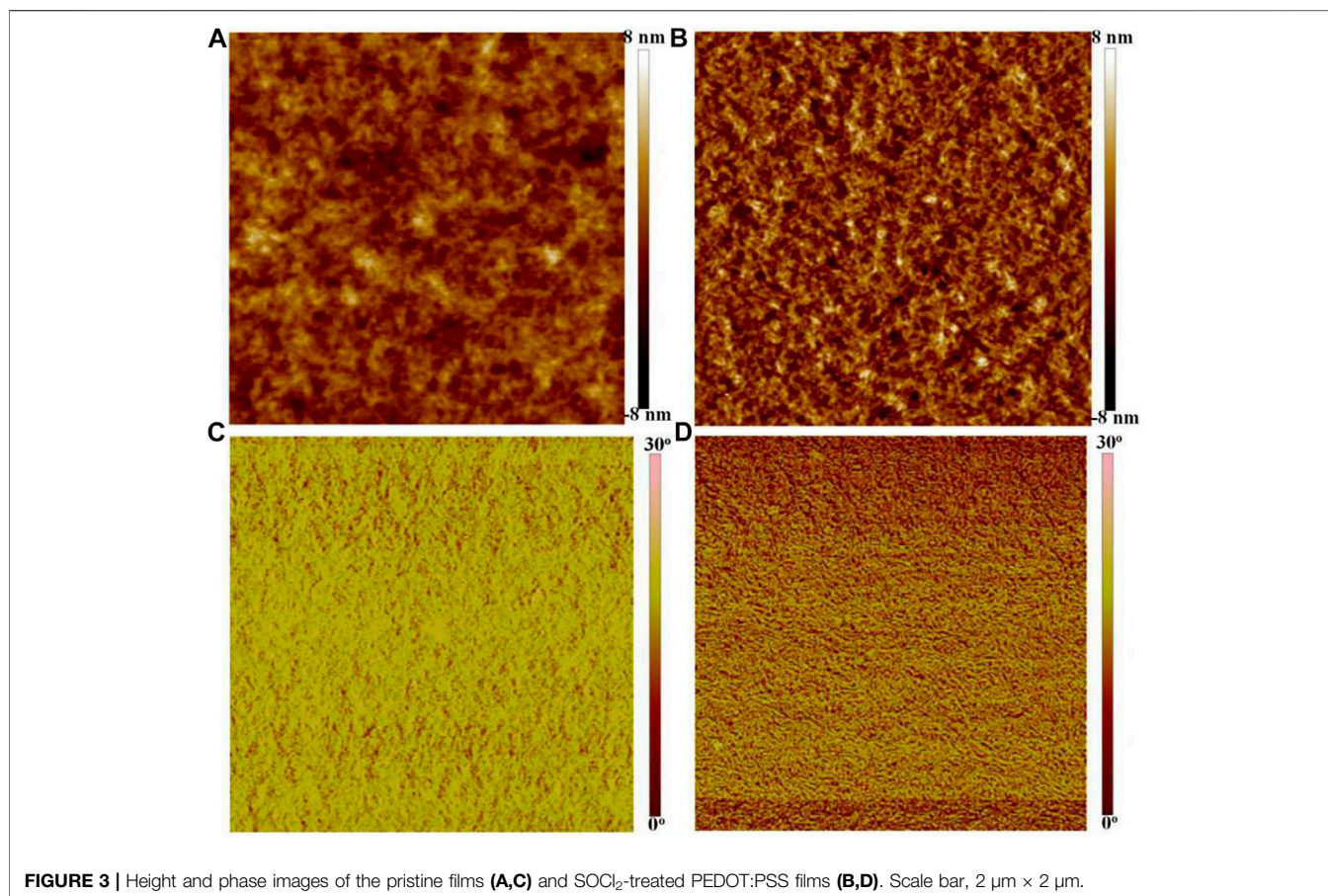
destroyed plastic underlying substrates, thereby unsuitable to prepare flexible PEDOT:PSS electrodes.

## Structure, Composition and Work Function of PEDOT:PSS Films

Figure 2C shows the Raman spectra of the PEDOT:PSS films, including the pristine ones and  $\text{SOCl}_2$ -treated ones. The strongest band between  $1,400$  and  $1,500 \text{ cm}^{-1}$  originated from the  $C_\alpha = C_\beta$  stretching vibration of the PEDOTs (Garreau et al., 1999). The  $C_\alpha = C_\beta$  vibration peak in Raman spectroscopy blue-shifted only  $1.6 \text{ cm}^{-1}$ . We found that this result was different from strong acid-treated PEDOT:PSS electrodes that exhibited a red-shift phenomenon. The result indicates a slight/rather limited change of the PEDOTs from quinoid structures to benzoid

structures. The peak at  $700 \text{ cm}^{-1}$  corresponds to the sym C–S–C vibrations in PEDOTs. Both peaks had a similar intensity and half-height width, thereby supporting the conclusion that there was no visible structure evolution of the PEDOTs.

To elucidate the effects of the  $\text{SOCl}_2$  treatment on the components of the PEDOT:PSS films, XPS spectra were conducted (see Figures 2D–F). The binding energy at  $201 \text{ eV}$  corresponds to the Cl2p peak. As shown in Figure 2D, the ratio of Cl in  $\text{SOCl}_2$  to total atoms is no more than 0.15 atom.% for the  $\text{SOCl}_2$ -treated films, suggesting little  $\text{SOCl}_2$  residuals on PEDOT:PSS surfaces; whereas a conventional treatment using high-concentration acids caused a large residual of acids that would affect the OSC efficiency. For example, the acid residual value was as high as 14.08 atom.% for the PEDOT:PSS electrodes with 85 wt.%



phosphoric acid ( $\text{H}_3\text{PO}_4$ ) treatment, and as-packaged flexible OSCs with the  $\text{H}_3\text{PO}_4$ -treated PEDOT:PSS electrodes showed a sharp decay of 17% when exposed in ambient air for 30 days (Fan et al., 2016).

For the pristine PEDOT:PSS films, the ratio of sulfur (S) atoms in sulfonate moieties of PSS to S atoms in thiophene rings of PEDOT (called  $S_{\text{PSS}}:S_{\text{PEDOT}}$ ) is 2.42:1; whereas, for the  $\text{SOCl}_2$ -treated films, the ratio is decreased to 2.07:1 (see **Figure 2E**), indicating a small removal of hydrophilic PSS from the PEDOT:PSS matrices. It ensures an intimate contact between the  $\text{SOCl}_2$ -treated PEDOT:PSS electrodes and PEDOT:PSS (Clevios P VP AI4083) HTLs. Besides, the content of the oxygen (O) atoms is decreased from 27.4 to 24.1 atom.% after the  $\text{SOCl}_2$  treatment (see **Figure 2F**), supporting the removals of the hydrophilic PSS components.

The energy levels of the PEDOT:PSS thin films were probed as well through UV photoelectron spectra, as shown in **Figure 2G**. **Figures 2H,I** show the low kinetic energy cutoff ( $E_{\text{cutoff}}$ ) and the Fermi levels ( $E_{\text{Fermi}}$ ) of the pristine- and  $\text{SOCl}_2$ -treated PEDOT:PSS films. The  $\text{SOCl}_2$ -treated films exhibited a work function of 4.89 eV that was higher than that (4.82 eV) of the pristine ones. The higher work function was probably attributed to the strong electron-withdrawing Cl groups of the  $\text{SOCl}_2$  molecules. It allows a formation of Ohmic contacts and is favored for hole transport from photo-active

layers of normal OSCs to the PEDOT:PSS electrodes treated by  $\text{SOCl}_2$ .

### Morphology and Stability of PEDOT:PSS Films

**Figure 3** shows the height and phase images of the PEDOT:PSS films through SPM. As shown in **Figure 3A**, the pristine PEDOT:PSS films with a root mean square (RMS) roughness of 1.32 nm exhibited an inferior phase-separated morphology. After the  $\text{SOCl}_2$  treatment, the PEDOT:PSS films with a higher RMS roughness of 1.95 nm showed the physically continuous and homogeneous networks that consisted of rich expanded/coiled chains for a free charge carrier hopping (**Figure 3B**). As shown in the phase image (**Figure 3C**), for the pristine films, the phases of the tip vibration are  $16^\circ$ – $23^\circ$  slower than that of the driving signals; whereas, for the  $\text{SOCl}_2$ -treated PEDOT:PSS thin films, plenty of phases of the tip vibration are no more than  $15^\circ$  slower than that of the driving signals (**Figure 3D**), suggesting a homogeneous and smooth thin film. The results demonstrate a much better phase-segregated morphology of the PEDOT:PSS thin films induced by the  $\text{SOCl}_2$  treatment.

PEDOT:PSS is prone to absorb water from the surrounding humid environments owing to the hygroscopic behavior of PSS and PSSH, thus potentially rendering the CPs vulnerable in

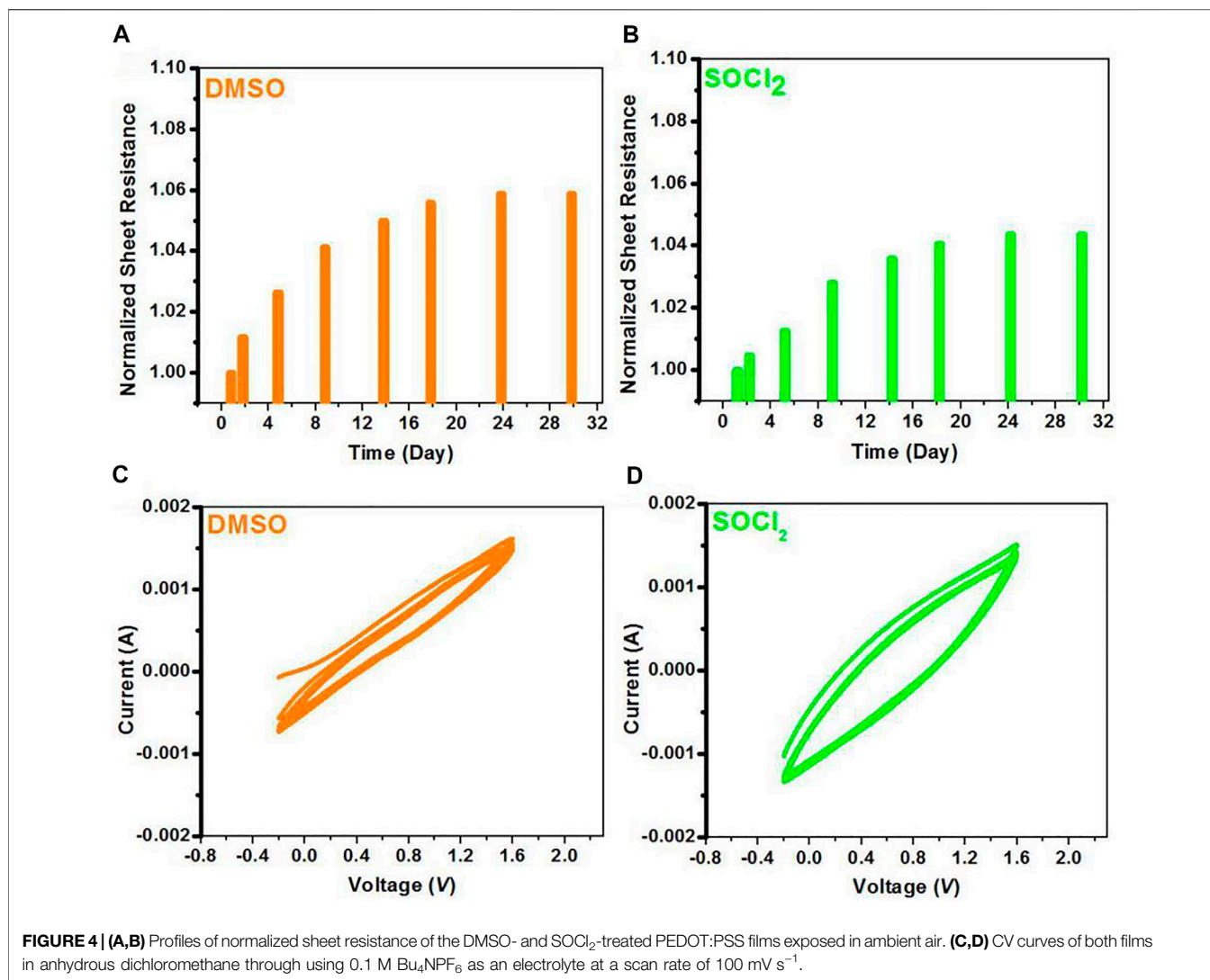


**FIGURE 4 | (A,B)** Profiles of normalized sheet resistance of the DMSO- and  $\text{SOCl}_2$ -treated PEDOT:PSS films exposed in ambient air. **(C,D)** CV curves of both films in anhydrous dichloromethane through using 0.1 M  $\text{Bu}_4\text{NPF}_6$  as an electrolyte at a scan rate of  $100 \text{ mV s}^{-1}$ .

ambient air. Volume expansion of PEDOT:PSS occurred in the ambient air would affect the charge hopping of the PEDOT:PSS films. Here, we investigated both electrical and electrochemical stabilities of the PEDOT:PSS films with 6 vol.% DMSO pre-treatments and the  $\text{SOCl}_2$  post-treatments. Note that both films were exposed in the ambient air (temperature:  $20^\circ\text{C}$ – $26^\circ\text{C}$ ; relative humidity: 60%–70%). **Figures 4A,B** show the normalized sheet resistance of the PEDOT:PSS thin films treated by DMSO and  $\text{SOCl}_2$ , respectively, in the ambient air for 30 days. An increase of 5.88% in  $R_{\text{sq}}$  was observed for the DMSO-treated PEDOT:PSS thin films, whereas an increase of 4.36% in  $R_{\text{sq}}$  was observed for the  $\text{SOCl}_2$ -treated PEDOT:PSS films. The limited increase in square resistance indicates a better air stability of the  $\text{SOCl}_2$ -treated PEDOT:PSS films. The promoted electrical stability of the  $\text{SOCl}_2$ -treated PEDOT:PSS films was mostly attributed to 1) the less components of hydrophilic and insulating PSS components in PEDOT:PSS matrices and 2) the homogeneous and better phase-segregated morphology that potentially restrained the absorption of moisture and volume expansion.

Furthermore, the electrochemical behaviors of the PEDOT:PSS thin films were investigated through cyclic voltammetry (CV), as shown in **Figures 4C,D**. In the CV tests, the PEDOT:PSS thin films were spin-coated on ITO working electrodes in 0.1 M  $\text{Bu}_4\text{NPF}_6$  (in  $\text{CH}_2\text{Cl}_2$ ) solutions. The PEDOT:PSS electrodes with the  $\text{SOCl}_2$  treatment had the stable reversibility during the oxidation–reduction process for 10 cycles, probably due to the less PSS components and the improved electrical conductivity. We found that the charge capacity of the  $\text{SOCl}_2$ -treated PEDOT:PSS thin films was larger than that of the DMSO-treated PEDOT:PSS thin films, suggesting more electron transferring in the doping and dedoping processes. The results demonstrate a better electrochemical stability of the PEDOT:PSS films achieved by the  $\text{SOCl}_2$  treatment.

## Photovoltaic Performances of Flexible OSCs

We fabricated the solution-processed flexible OSCs on the basis of the PEDOT:PSS transparent electrodes with the  $\text{SOCl}_2$

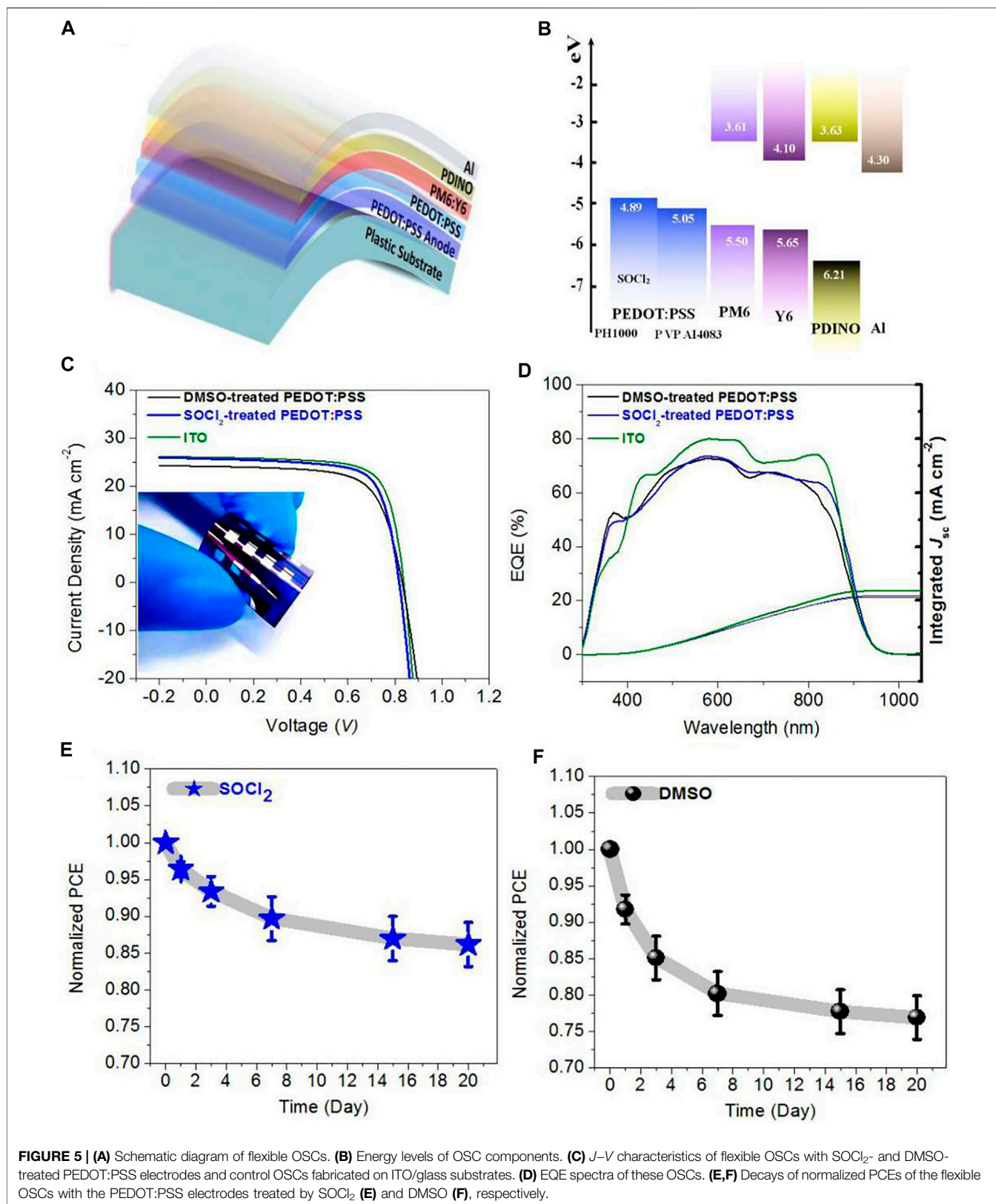


**FIGURE 5 | (A)** Schematic diagram of flexible OSCs. **(B)** Energy levels of OSC components. **(C)** *J*-*V* characteristics of flexible OSCs with SOCl<sub>2</sub>- and DMSO-treated PEDOT:PSS electrodes and control OSCs fabricated on ITO/glass substrates. **(D)** EQE spectra of these OSCs. **(E,F)** Decays of normalized PCEs of the flexible OSCs with the PEDOT:PSS electrodes treated by SOCl<sub>2</sub> **(E)** and DMSO **(F)**, respectively.

**TABLE 1** | Photovoltaic parameters of flexible OSCs based on PEDOT:PSS electrodes and rigid OSCs based on ITO electrodes.

Transparent electrode	Treatment	$V_{oc}$ [V]	$J_{sc}$ [ $\text{mA cm}^{-2}$ ]	Fill factor	PCE [%]
PEDOT:PSS	$\text{SOCl}_2$	0.818 ( $\pm 0.005$ )	25.73 ( $\pm 0.22$ )	0.719 ( $\pm 0.004$ )	15.12 ( $\pm 0.20$ )
PEDOT:PSS	DMSO	0.821 ( $\pm 0.005$ )	24.21 ( $\pm 0.24$ )	0.688 ( $\pm 0.005$ )	13.69 ( $\pm 0.26$ )
ITO	none	0.835 ( $\pm 0.004$ )	26.06 ( $\pm 0.19$ )	0.730 ( $\pm 0.04$ )	15.89 ( $\pm 0.08$ )

treatment. **Figure 5A** illustrates the flexible OSC structure, that is, PET (100  $\mu\text{m}$ )/ $\text{SOCl}_2$ -treated PEDOT:PSS (Clevios PH1000, 70 nm)/PEDOT:PSS (Clevios P VP AI4083, 25 nm)/PM6:Y6 (150 nm)/PDINO (10 nm)/Al (100 nm). The energy levels of the solar cell components are shown in **Figure 5B**. The good matching in energy levels among the  $\text{SOCl}_2$ -treated PEDOT:PSS electrodes, PEDOT:PSS (P VP AI4083) HTLs, and PM6 allowed an efficient hole transfer into the PEDOT:PSS electrodes. **Figure 5C** shows the  $J$ - $V$  characteristics of the three kinds of OSCs, including 1) flexible ones with the  $\text{SOCl}_2$ -treated PEDOT:PSS electrodes, 2) flexible ones with the conventional 6 vol.% DMSO pre-treatments, and 3) rigid ones fabricated on ITO (110 nm)/glass substrates. It presented that the flexible OSCs with the  $\text{SOCl}_2$ -treated PEDOT:PSS electrodes yielded an average PCE of 15.12% with a high fill factor (FF) of 0.719 and a short-circuit current density ( $J_{sc}$ ) of 25.73  $\text{mA cm}^{-2}$  under the illumination of AM 1.5G, 100  $\text{mW cm}^{-2}$ . The PCE is higher than that (PCE:13.69%) of the control flexible OSCs with the DMSO-treated PEDOT:PSS electrodes that showed a  $J_{sc}$  of 24.21  $\text{mA cm}^{-2}$  and a FF of 0.688. The higher PCE was mostly attributed to the higher electrical conductivity, suitable work function, and better phase-separated morphology of the  $\text{SOCl}_2$ -treated PEDOT:PSS electrodes for an efficient charge collection. It is worth mentioning that the match (4.89, 5.05, and 5.50 eV) in energy levels of the  $\text{SOCl}_2$ -treated electrodes, HTLs, and PM6 and the homogeneous morphology of the  $\text{SOCl}_2$ -treated electrodes allow efficient hole transfer into the as-treated PEDOT:PSS electrodes for maximizing the PCE of the flexible OSCs. Furthermore, the PCE of the optimal flexible OSCs is nearly comparable to that (PCE: 15.89%) of the control rigid OSCs fabricated on ITO (110 nm)/glass substrates that exhibited a high FF of 0.730 and a high  $J_{sc}$  of 26.06  $\text{mA cm}^{-2}$ . **Table 1** summarizes the performance data of the flexible and rigid OSCs for reference.

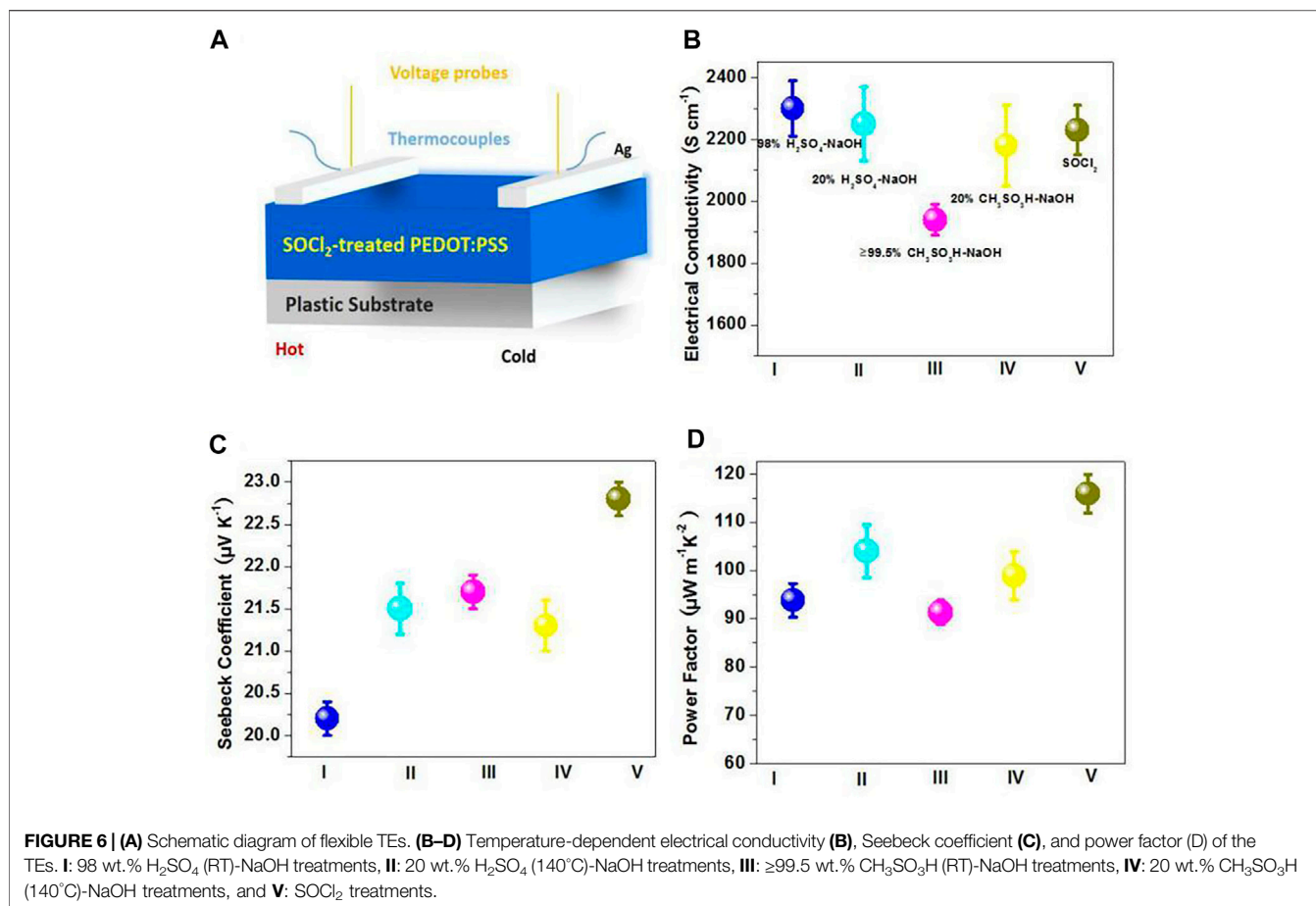
**Figure 5D** shows the EQE of the solution-processed flexible OSCs with the  $\text{SOCl}_2$ - and DMSO-treated PEDOT:PSS electrodes and the control rigid OSCs fabricated on the ITO/glass substrates. The maximum EQE value of the optimal flexible OSCs with the  $\text{SOCl}_2$ -treated PEDOT:PSS electrodes reached 84.6% at  $\lambda = 580$  nm and 77.7% at  $\lambda = 700$  nm, which demonstrated the high integrated  $J_{sc}$  of 25.11  $\text{mA cm}^{-2}$ . In contrast, for the control flexible OSCs with the DMSO-treated PEDOT:PSS electrodes, the EQE value at 580 nm reached 79.8% at  $\lambda = 580$  nm and 73.8% at  $\lambda = 700$  nm, which showed an integrated  $J_{sc}$  of 23.82  $\text{mA cm}^{-2}$ ; whereas the control rigid OSCs fabricated on the ITO/glass showed the integrated  $J_{sc}$  as high as 25.70  $\text{mA cm}^{-2}$ . It can be seen that the EQE values are nearly consistent with the measured  $J_{sc}$  for all that flexible and rigid solar cells. The  $\text{SOCl}_2$  treatment raised the light utilization especially in the

wavelengths of 500–900 nm. Therefore, the  $\text{SOCl}_2$ -treated PEDOT:PSS thin films are suitable for efficient flexible OSCs fabrications as a flexible transparent electrode. We also investigated the stability of both flexible devices with  $\text{SOCl}_2$ - and DMSO-treated PEDOT:PSS electrodes as a function of storage time. **Figures 5E,F** present the profiles of the normalized PCE of the flexible OSCs versus storage time. Obviously, the flexible OSCs with the  $\text{SOCl}_2$ -treated PEDOT:PSS electrodes still maintain  $\sim 86.2\%$  of the initial PCE after the storage for 20 days in the glove boxes, whereas the flexible OSCs with the DMSO-treated PEDOT:PSS electrodes just held  $\sim 76.9\%$  of the initial PCE value. The improved device stability was attributed to the better electrochemical behaviors of the  $\text{SOCl}_2$ -treated PEDOT:PSS electrodes and the raised electrical stability, as shown in **Figure 4**.

## Thermoelectric Performances of Flexible TEs

Furthermore, to demonstrate the promising applications of the  $\text{SOCl}_2$ -treated PEDOT:PSS thin films, we fabricated the flexible polymeric TEs on the basis of the PEDOT:PSS as active thermoelectric layers. The PEDOT:PSS TE device structure is illustrated in **Figure 6A**. **Figures 6B–D** show the temperature-dependent electrical conductivity, Seebeck coefficient, and PF of the PEDOT:PSS TEs, including 1) the flexible TEs based on the  $\text{SOCl}_2$ -treated PEDOT:PSS films and 2) the four kinds of control rigid TEs based on the PEDOT:PSS films with the  $\text{H}_2\text{SO}_4$  and sodium hydroxide ( $\text{H}_2\text{SO}_4$ -NaOH) multistep treatments and the  $\text{CH}_3\text{SO}_3\text{H}$  and NaOH ( $\text{CH}_3\text{SO}_3\text{H}$ -NaOH) multistep treatments. The conventional PEDOT:PSS films with strong acid treatments commonly showed a poor Seebeck coefficient and a limited PF (Fan et al., 2017). To increase the Seebeck coefficient and PF, the following NaOH base treatment was required to treat the acid-treated PEDOT:PSS films. As shown in **Figure 6B**, through using the  $\text{SOCl}_2$  treatment, the electrical conductivity of the flexible PEDOT:PSS thin films was enhanced from 0.3 to 2,230  $\text{S cm}^{-1}$ . The electrical conductivity of the flexible  $\text{SOCl}_2$ -treated films is higher than that (1,940  $\text{S cm}^{-1}$ ) of the  $\geq 99.5$  wt.%  $\text{CH}_3\text{SO}_3\text{H}$ -NaOH-treated films but slightly lower than that (2,300  $\text{S cm}^{-1}$ ) of the 98 wt.% strong acid (i.e.,  $\text{H}_2\text{SO}_4$ )-NaOH-treated films. Note that the  $\text{H}_2\text{SO}_4$ -treated PEDOT:PSS thin films were prepared on glass substrates rather than plastic underlying substrates, because of a large-domain damage of  $\text{H}_2\text{SO}_4$  to most of plastic substrates; whereas the  $\text{SOCl}_2$  treatment is compatible with a flexible electrode solution manufacturing. The results demonstrate a better electrical conductivity of the  $\text{SOCl}_2$ -treated PEDOT:PSS





thin films. In terms of Seebeck coefficient, the PEDOT:PSS films with acid-NaOH treatment on glass substrates exhibited a Seebeck coefficient between 20.2 and 21.7  $\mu\text{V K}^{-1}$ ; whereas the SOCl<sub>2</sub> treatment at room temperature induced a considerably high Seebeck coefficient of 22.8  $\mu\text{V K}^{-1}$ . As a result, the SOCl<sub>2</sub>-treated PEDOT:PSS flexible thin films yielded the best PF value of 115.9  $\mu\text{W m}^{-1} \text{K}^{-2}$ , which outperformed these control rigid PEDOT:PSS TEs that had a relatively low PF of 91.3  $\mu\text{W m}^{-1} \text{K}^{-2}$  for ≥99.5 wt.% CH<sub>3</sub>SO<sub>3</sub>H (RT)-NaOH treatments; 93.8  $\mu\text{W m}^{-1} \text{K}^{-2}$  for 98 wt.% H<sub>2</sub>SO<sub>4</sub> (RT)-NaOH treatments; 98.9  $\mu\text{W m}^{-1} \text{K}^{-2}$  for 20 wt.% CH<sub>3</sub>SO<sub>3</sub>H-NaOH treatments; and 104.0  $\mu\text{W m}^{-1} \text{K}^{-2}$  for 20 wt.% H<sub>2</sub>SO<sub>4</sub>-NaOH treatments, respectively. Note that the diluted acid treatments of 20 wt.% CH<sub>3</sub>SO<sub>3</sub>H and 20 wt.% H<sub>2</sub>SO<sub>4</sub> were conducted at a higher temperature of 140°C. The results demonstrate that the simple SOCl<sub>2</sub> treatment is superior to these multistep acid-NaOH treatments in terms of raising Seebeck coefficient and PF.

The mechanism for the TE property enhancement of the PEDOT:PSS films treated by SOCl<sub>2</sub> may be explored as below. In our recent works, the conventional CF<sub>3</sub>SO<sub>3</sub>H (Wan et al., 2021) and HClO<sub>4</sub> (Wan et al., 2020a) treatments commonly enabled a doped PEDOT:PSS film, leading to a blue shift of the Raman peak at 1,430–1,440  $\text{cm}^{-1}$ . When the pristine PEDOT:PSS film was subject to the SOCl<sub>2</sub> treatment, a blue shift of the Raman

peak at 1,430–1,440  $\text{cm}^{-1}$  was observed here, suggesting a dedoping process of PEDOTs and a localization of the positive charges on PEDOTs. Many protons would be removed from the PEDOTs during the SOCl<sub>2</sub> processing, resulting in a lower charge concentration and thus enhancing the Seebeck coefficient of the PEDOT:PSS thin films. In recent literature, a rigid PEDOT:PSS/glass sample with optimized H<sub>2</sub>SO<sub>4</sub> soaking treatments and optimized base treatments exhibited a record-high PF of 334  $\mu\text{W m}^{-1} \text{K}^{-2}$  due to an inspiring Seebeck coefficient. The PF of our flexible PEDOT:PSS thin films lagged behind the record-high PF of the rigid and opaque PEDOT:PSS/glass samples that required a precise optimization of H<sub>2</sub>SO<sub>4</sub> soaking treatments and base treatments. However, the H<sub>2</sub>SO<sub>4</sub> treatments caused a large-domain damage to most of flexible plastic substrates, thereby unsuitable to prepare flexible PEDOT:PSS TEs; meanwhile, the following NaOH base treatments changed the color of the PEDOT:PSS films from light blue to dark blue, therefore, hampering the realization of highly transparent TE devices. In this work, the flexible TEs based on the SOCl<sub>2</sub>-treated PEDOT:PSS thin films not only have the advantages of simple solution-treatment/manufacturing, good flexibility, and highly optical transmittance but also are desirable to realize the kinds of

flexible devices, such as flexible and transparent TEs, flexible OSCs, and integrated electronics involving flexible TEs and OSCs.

## CONCLUSION

In summary, we demonstrated the high-performance flexible OSCs and flexible TEs on the basis of the  $\text{SOCl}_2$ -treated PEDOT:PSS electrodes. The  $\text{SOCl}_2$  treatment enabled a homogeneous and smooth PEDOT:PSS electrode with highly electrical conductivity of  $2,230 \text{ S cm}^{-1}$  and Seebeck coefficient of  $22.8 \mu\text{V K}^{-1}$ . The resultant flexible OSCs yielded the high PCE of 15.12%. It is almost attributed to the  $\text{SOCl}_2$  treatment that endowed the PEDOT:PSS electrodes with highly optical and electrical characteristics, homogeneous and smooth morphology, and high work function (4.89 eV). Besides, the flexible PEDOT:PSS TEs not only had the merit of high transmittance but also yielded a PF of  $115.9 \mu\text{W m}^{-1} \text{ K}^{-2}$ , which was higher than that ( $91.3\text{--}104.0 \mu\text{W m}^{-1} \text{ K}^{-2}$ ) of the four kinds of rigid PEDOT:PSS TEs with acid and NaOH multistep treatments. The work opens a venue to realize more efficient solution-processed flexible OSCs and flexible TEs that convert both luminous and thermal energies to electricity.

## REFERENCES

- Chen, X., Xu, G., Zeng, G., Gu, H., Chen, H., Xu, H., et al. (2020). Realizing Ultrahigh Mechanical Flexibility and >15% Efficiency of Flexible Organic Solar Cells via a "Welding" Flexible Transparent Electrode. *Adv. Mater.* 32, e1908478. doi:10.1002/adma.201908478
- Fan, X. (2021). Doping and Design of Flexible Transparent Electrodes for High-Performance Flexible Organic Solar Cells: Recent Advances and Perspectives. *Adv. Funct. Mater.* 31, 2009399. doi:10.1002/adfm.202009399
- Fan, X., Nie, W., Tsai, H., Wang, N., Huang, H., Cheng, Y., et al. (2019). PEDOT:PSS for Flexible and Stretchable Electronics: Modifications, Strategies, and Applications. *Adv. Sci.* 6, 1900813. doi:10.1002/advs.201900813
- Fan, X., Wang, J., Wang, H., Liu, X., and Wang, H. (2015). Bendable ITO-free Organic Solar Cells with Highly Conductive and Flexible PEDOT:PSS Electrodes on Plastic Substrates. *ACS Appl. Mater. Inter.* 7, 16287–16295. doi:10.1021/acsami.5b02830
- Fan, X., Wen, R., Xia, Y., Wang, J., Liu, X., Huang, H., et al. (2020). Vacuum-Free, All-Solution, and All-Air Processed Organic Photovoltaics with over 11% Efficiency and Promoted Stability Using Layer-By-Layer Codoped Polymeric Electrodes. *Solar RRL* 4, 1900543. doi:10.1002/solr.201900543
- Fan, X., Xu, B., Liu, S., Cui, C., Wang, J., and Yan, F. (2016). Transfer-Printed PEDOT:PSS Electrodes Using Mild Acids for High Conductivity and Improved Stability with Application to Flexible Organic Solar Cells. *ACS Appl. Mater. Inter.* 8, 14029–14036. doi:10.1021/acsami.6b01389
- Fan, Z., Li, P., Du, D., and Ouyang, J. (2017). Significantly Enhanced Thermoelectric Properties of PEDOT:PSS Films through Sequential Post-Treatments with Common Acids and Bases. *Adv. Energy Mater.* 7, 1602116. doi:10.1002/aenm.201602116
- Garreau, S., Louarn, G., Buisson, J. P., Froyer, G., and Lefrant, S. (1999). *In Situ* Spectroelectrochemical Raman Studies of Poly(3,4-Ethylenedioxythiophene) (PEDT). *Macromolecules* 32, 6807–6812. doi:10.1021/ma9905674
- Jiang, Q., Sun, H., Zhao, D., Zhang, F., Hu, D., Jiao, F., et al. (2020). High Thermoelectric Performance in n-Type Perylene Bisimide Induced by the Soret Effect. *Adv. Mater.* 32, 2002752. doi:10.1002/adma.202002752
- Khan, Z. U., Bubnova, O., Jafari, M. J., Brooke, R., Liu, X., Gabrielson, R., et al. (2015). Acido-basic Control of the Thermoelectric Properties of Poly(3,4-

## DATA AVAILABILITY STATEMENT

The original contributions presented in the study are included in the article/supplementary material. Further inquiries can be directed to the corresponding authors.

## AUTHOR CONTRIBUTIONS

XF designed the research and wrote the manuscript. JW fabricated the devices and contributed to the optical and electrical characteristics, surface morphology characteristics, and the XPS. YL and PL conducted the thermoelectric performances. TZ, KH, HH, KK, and LQ contributed analytic tools and provided valuable suggestions and discussions.

## FUNDING

We are grateful for the programs supported by Ningbo natural science foundation (2021J195) and Zhejiang Provincial Natural Science Foundation of China under Grant No. LGG22F040003.

- Ethylenedioxythiophene)tosylate (PEDOT-Tos) Thin Films. *J. Mater. Chem. C* 3, 10616–10623. doi:10.1039/c5tc01952d
- Kim, N., Kee, S., Lee, S. H., Lee, B. H., Kahng, Y. H., Jo, Y.-R., et al. (2014). Highly Conductive PEDOT:PSS Nanofibrils Induced by Solution-Processed Crystallization. *Adv. Mater.* 26, 2268–2272. doi:10.1002/adma.201304611
- Kim, Y. H., Sachse, C., Machala, M. L., May, C., Müller-Meskamp, L., and Leo, K. (2011). Highly Conductive PEDOT:PSS Electrode with Optimized Solvent and Thermal Post-Treatment for ITO-free Organic Solar Cells. *Adv. Funct. Mater.* 21, 1076–1081. doi:10.1002/adfm.201002290
- Li, Q., Deng, M., Zhang, S., Zhao, D., Jiang, Q., Guo, C., et al. (2019). Synergistic Enhancement of Thermoelectric and Mechanical Performances of Ionic Liquid LITFSI Modulated PEDOT Flexible Films. *J. Mater. Chem. C* 7, 4374–4381. doi:10.1039/C9TC00310J
- Meng, W., Ge, R., Li, Z., Tong, J., Liu, T., Zhao, Q., et al. (2015). Conductivity Enhancement of PEDOT:PSS Films via Phosphoric Acid Treatment for Flexible All-Plastic Solar Cells. *ACS Appl. Mater. Inter.* 7, 14089–14094. doi:10.1021/acsami.5b03309
- Na, S.-I., Kim, S.-S., Jo, J., and Kim, D.-Y. (2008). Efficient and Flexible ITO-free Organic Solar Cells Using Highly Conductive Polymer Anodes. *Adv. Mater.* 20, 4061–4067. doi:10.1002/adma.200800338
- Park, H., Lee, S. H., Kim, F. S., Choi, H. H., Cheong, I. W., and Kim, J. H. (2014). Enhanced Thermoelectric Properties of PEDOT:PSS Nanofilms by a Chemical Dedoping Process. *J. Mater. Chem. A* 2, 6532–6539. doi:10.1039/C3TA14960A
- Qu, T., Zou, L., Chen, J., Shi, X., Zhang, T., Li, L., et al. (2020). Biomimetic Electrodes for Flexible Organic Solar Cells with Efficiencies over 16%. *Adv. Opt. Mater.* 8, 2000669. doi:10.1002/adom.202000669
- Reyes-Reyes, M., and López-Sandoval, R. (2018). Optimizing the Oxidation Level of PEDOT Anode in Air-PEDOT Battery. *Org. Elect.* 52, 364–370. doi:10.1016/j.orgel.2017.11.016
- Snyder, G. J., and Toberer, E. S. (2008). Complex Thermoelectric Materials. *Nat. Mater.* 7, 105–114. doi:10.1038/nmat2090
- Song, W., Fan, X., Xu, B., Yan, F., Cui, H., Wei, Q., et al. (2018). All-Solution-Processed Metal-oxide-free Flexible Organic Solar Cells with over 10% Efficiency. *Adv. Mater.* 30, e1800075. doi:10.1002/adma.201800075
- Sun, Y., Chang, M., Meng, L., Wan, X., Gao, H., Zhang, Y., et al. (2019). Flexible Organic Photovoltaics Based on Water-Processed Silver Nanowire Electrodes. *Nat. Electron.* 2, 513–520. doi:10.1038/s41928-019-0315-1

- Tritt, T. M., and Subramanian, M. A. (2006). Thermoelectric Materials, Phenomena, and Applications: A Bird's Eye View. *MRS Bull.* 31, 188–198. doi:10.1557/mrs2006.44
- Wan, J., Xia, Y., Fang, J., Zhang, Z., Xu, B., Wang, J., et al. (2021). Solution-Processed Transparent Conducting Electrodes for Flexible Organic Solar Cells with 16.61% Efficiency. *Nanomicro Lett.* 13, 44. doi:10.1007/s40820-020-00566-3
- Wan, J., Fan, X., Huang, H., Wang, J., Zhang, Z., Fang, J., et al. (2020b). Metal Oxide-free Flexible Organic Solar Cells with 0.1 M Perchloric Acid Sprayed Polymeric Anodes. *J. Mater. Chem. A* 8, 21007–21015. doi:10.1039/D0TA07934K
- Wan, J., Wen, R., Xia, Y., Dai, M., Huang, H., Xue, L., et al. (2020a). All Annealing-free Solution-Processed Highly Flexible Organic Solar Cells. *J. Mater. Chem. A* 9, 5425–5433. doi:10.1039/D0TA11831A
- Wen, R., Huang, H., Wan, J., Wen, S., Wang, J., and Fan, X. (2021). High-Efficiency Stable Flexible Organic Solar Cells with PEDOT:PSS Electrodes via Superacid Fumigation Treatment. *Energy Technol.* 9, 2100595. doi:10.1002/ente.202100595
- Worfolk, B. J., Andrews, S. C., Park, S., Reinspach, J., Liu, N., Toney, M. F., et al. (2015). Ultrahigh Electrical Conductivity in Solution-Sheared Polymeric Transparent Films. *Proc. Natl. Acad. Sci. U.S.A.* 112, 14138–14143. doi:10.1073/pnas.1509958112
- Xia, Y., Sun, K., and Ouyang, J. (2012). Solution-Processed Metallic Conducting Polymer Films as Transparent Electrode of Optoelectronic Devices. *Adv. Mater.* 24, 2436–2440. doi:10.1002/adma.201104795
- Xiong, J., Jiang, F., Zhou, W., Liu, C., and Xu, J. (2015). Highly Electrical and Thermoelectric Properties of a PEDOT:PSS Thin-Film via Direct Dilution-Filtration. *RSC Adv.* 5, 60708–60712. doi:10.1039/C5RA07820B
- Xu, Y., Jia, Y., Liu, P., Jiang, Q., Hu, D., and Ma, Y. (2021). Poly(3,4-ethylenedioxythiophene) (PEDOT) as Promising Thermoelectric Materials and Devices. *Chem. Eng. J.* 404, 126552. doi:10.1016/j.cej.2020.126552
- Yao, J., Qiu, B., Zhang, Z. G., Xue, L., Wang, R., Zhang, C., et al. (2020). Cathode Engineering with Perylene-Diimide Interlayer Enabling over 17% Efficiency Single-junction Organic Solar Cells. *Nat. Commun.* 11, 2726. doi:10.1038/s41467-020-16509-w

**Conflict of Interest:** The authors declare that the research was conducted in the absence of any commercial or financial relationships that could be construed as a potential conflict of interest.

**Publisher's Note:** All claims expressed in this article are solely those of the authors and do not necessarily represent those of their affiliated organizations or those of the publisher, the editors, and the reviewers. Any product that may be evaluated in this article, or claim that may be made by its manufacturer, is not guaranteed or endorsed by the publisher.

Copyright © 2022 Wan, Fan, Li, Li, Zhang, Hui, Huang, Kang and Qian. This is an open-access article distributed under the terms of the Creative Commons Attribution License (CC BY). The use, distribution or reproduction in other forums is permitted, provided the original author(s) and the copyright owner(s) are credited and that the original publication in this journal is cited, in accordance with accepted academic practice. No use, distribution or reproduction is permitted which does not comply with these terms.